Characteristics of PPS-1350 type thrusters under increased discharge voltages and comparison with hybrid codes simulation results

IEPC-2005-136
Presented at the 29th International Electric Propulsion Conference, Princeton University, October 31 – November 4, 2005

L. Albarède[•] and A. Bouchoule[⊗]
Laboratoire GREMI, université d'Orléans 45067 Orléans France

A. Lazurenko[♣]
Laboratoire d'Aérothermique CNRS 45071 Orléans France

and

V. Kim and V. Kozlov and A. Skrylnikov[§]
RIAME Moscow Russia

Experimental characteristics of a standard PPS-1350 thruster and of a modified laboratory model are reported for extended operating voltages. The modified version was designed in order to allow a more effective control of the magnetic field across the thruster channel. The operation parameter ranges were (0-1000 V) for the discharge voltage, (1.5-5 mg/s) for the anodic Xe mass flow rate and (0.5- 4.5 kW) for the discharge power.

The performance data of the standard thruster show that specific impulse values (not taking into account the cathode mass flow) ~2870 s can be obtained under discharge power ~2 kW, discharge voltage ~800 V and anode mass flow rate ~2.77 mg/s. They suggest also that increasing specific impulse (i.e. voltage) under fixed discharge power encounters a limitation due to a significant reduction of thrust efficiency at low mass flow rate.

The exploration of the modified PPS-1350-MLM version show that this limitation is much less constraining for high specific impulse operation. At reduced mass flows, the ratio of the discharge current to the anodic mass flow equivalent current remains almost constant till mass flow rates ~2.5 mg/s, while it decreases significantly in the standard thruster version. The total ion current in the plume has been derived from RPA probe data, confirming this improved mass utilization efficiency: near 85% is obtained for thruster operation at 2.5 mg/s and ~700 V.

The study of the PPS 1350 MLM included measurements of local plasma parameters, by using near wall probes. The experimental results were compared with simulation code data, obtained by using the hybrid code developed by CPAT laboratory. In spite of some discrepancies, both data suggest a significant increase of the electron energies at high voltage operation, leading to an improvement of the mass utilization efficiency.

[•] Post-doc., albarede@cnrs-orleans.fr
[⊗] Prof., andre.bouchoule@univ-orleans.fr
[♣] Post-doc., lazurenk@cnrs-orleans.fr

Nomenclature

c_θ = coefficient of divergence
e = electron charge
E_i = ions energy
Eff = Thrust efficiency
g = gravitational constant
I_d = discharge current
I_e = electron current component
I_i = ionic current component
I_i^+ = single charged ionic current component
I_i^{2+} = doubly charged ionic current component
I_m = equivalent anode current
Isp = specific impulse
$\dot{m}_a$ = anode mass flow rate
$\dot{m}_i$ = ion mass flow
$\dot{m}_i^+$ = single charged ions mass flow
$\dot{m}_i^{2+}$ = doubly charged ions mass flow
M = atom mass of xenon
M_{Xe} = molar mass of xenon
$\aleph_A$ = Avogadro number
T = thrust
U_d = applied discharge voltage
v_i^+ = single charge ion velocity
v_{i0}^+ = single charge ion flux velocity on the axis
ΔU = losses of potential
γ = ionization efficiency
θ = divergence
δ = coefficient of divergence effect
Φ_i^+ = ion flux
Φ_{i0}^+ = ion flux on the symmetric axis

Introduction

Hall thrusters of the SPT type are presently successfully used in the Russian and Western space technologies and there are definite plans to extend their application in the future[1-2], with expected improvements on operational power, thrust, specific impulse and life time. In particular it is attractive to develop SPTs with significantly increased specific impulse, i.e. operated at increased discharge voltages. Previous studies of SPT performances under increased discharge voltages[3-7] evidenced already the possibility to achieve specific impulse values ~3000s and higher. But achieving high specific impulse at moderate thruster power, of interest for large life times, requires further studies and design improvements and is the main aim of this paper. The development of simulation models and codes as reliable tools for physical analysis and performance prediction is a general and important issue and is also considered in this contribution.
Both a standard PPS-1350 thruster and a modified laboratory version (PPS-1350-MLM) have been investigated in a broad voltage range, including values as high as 1000V. The PPS-1350-MLM has a magnetic design allowing magnetic field topology different from the standard thruster. Significantly different integral characteristics have been evidenced for the MLM model. The study of this last thruster included also local plasma parameter measurements along the external discharge chamber wall. This rather extensive set of experimental data represents a useful basis for comparison with simulation models and codes. Preliminary results are given here for such a comparison between code and experimental data, based on the 2D hybrid code developed at CPAT [8-9] laboratory.

I. Methodology

A) PPS-1350 standard version

The standard **PPS-1350** developed by SNECMA is used in the lunar ESA mission SMART-1 (Ref. 2). Performance data have already been presented[10] along with comprehensive physical insights into the thruster operation[11]. Here, a performance overview for the comparison with the **PPS-1350-MLM** is given. Its characteristics have been investigated in the French national test facility PIVOINE (see Ref. 12) characterized by the chamber size (2.2m diameter - 4m length) and operating pressure (2.10^{-5} mBar for a Xe mass flow rate of 5 mg/s).

The integral data (current, thrust) of this thruster was recorded:

- With a cathode Xe flow proportional to the anode one : $\dot{m}_c = 0.082.\dot{m}_a$
- With the same current in internal and external magnetic coil, adjusted for minimizing the thruster current at the operating point (voltage and mass flow)
- When the discharge current is stabilized for at least 15 minutes

A 16 channels, 250 kHz rate acquisition unit stored a large set of information for each operating point, including anode and cathode line currents and voltages (referenced to the grounded vacuum chamber). Thrust values are obtained by using a thrust balance, with an absolute accuracy better than 1mN as allowed by the calibration procedure.

B) PPS-1350 MLM upgraded version

The standard PPS-1350 was designed for optimal operation at nominal voltage of 350V. In order to achieve a stable higher voltage operation the magnetic field is increased but this model encounters design limitations. A higher flux in the magnetic circuit was allowed in the upgraded version, in order to avoid such limitations. Moreover the topology of magnetic field was modified, with an attempt to reduce the ion flux onto the ceramics surface by a better control of the ionization area location and of the divergence of the ion beam.
The study of the PPS 1350 MLM was performed at the RIAME MAI test facility[3] where the vacuum chamber (2m diameter, 6 m length) is equipped with two diffusion pumps (working pressure $6.6 \cdot 10^{-5}$ mbar for an Xe mass-flow of 5 mg/s). The xenon flows in anode and cathode lines were separately controlled by MKS controllers, the cathode gas flow being fixed to 0.45mg/s in all reported experiments.
Internal (central), external and additional magnetization coil currents were controlled by three independent stabilized power supply sources. Before recording experimental data the thruster was outgassed by several hours in vacuum conditions followed by a preparative run of ~1 hour duration at discharge power close to ~1kW.
An estimation of the total current I_i leaving the thruster was derived from measurements of the ion current density along a semi-circle (radius ~0.7m) centered on the axis of the channel exit plane. These data were obtained up to off-axis angles ± 90° and the total ion current was derived through the usual assumption of azimutal symmetry of the plume. In order to avoid the collection of ions from the secondary plasma the RPA retarding potential was set at -50V relative to the cathode potential. It means that the given values of the total ion current could be underestimated but, inversely, it is worth to mention that the secondary electron flow leaving the RPA collector was not suppressed in these measurements.

C) Local parameters measurements

A set of the near wall probes (**Fig. 1**), installed along the external ceramic wall, was used to estimate the local plasma parameters distribution inside the accelerating channel. Together with the thruster outgassing procedure, a probe cleaning sequence was applied before probe recordings, by setting the probe potentials at negative values with respect to floating potential. Methodical experiment had shown also that insertion of probes does not disturb thruster integral parameters significantly but optimum magnetization currents were slightly changed. Therefore the integral and local parameters were determined with probes during the same experiment.
The probe electrical characteristics were acquired by using a signal registration circuit allowing a significant reduction of the noise related to thruster operation. This filtering technique was the most efficient in the near anode zone of the channel. The ion current and the floating potential are the most reliable probe data, the electron energy distribution and the plasma potential being more questionable, especially in the part of channel where plasma parameter gradients and fluctuation level were large (within the accelerating layer). Nevertheless it seems possible to use these results with some confidence: they appear to be in good correspondence with other experimental insights on the channel, such as the erosion trace lengths after several hours of thruster operation in constant conditions.

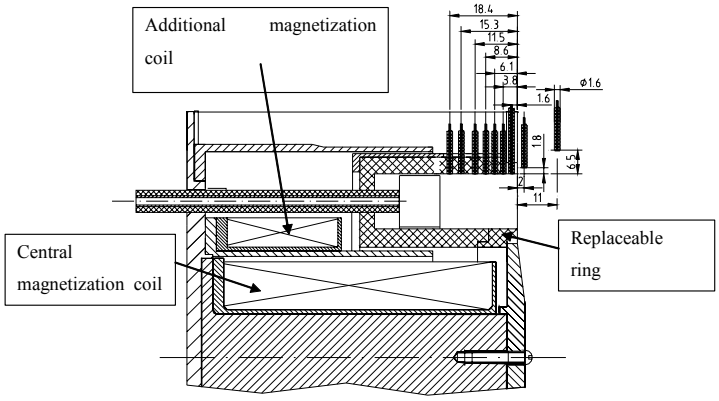

Fig. 1 Schematics of the probes positions relative to the discharge chamber

II. Performances comparison and discussion

A) Experimental data

In the data presented below, the specific impulse and the efficiency are given without accounting for both the cathode mass flow rate and the power consumed in the magnetic coils.

Specific impulse: $Isp = \frac{T}{\dot{m}_a g}$ Efficiency: $Eff = \frac{T^2}{2U_d I_d \dot{m}_a}$

1) Discharge current and thrust

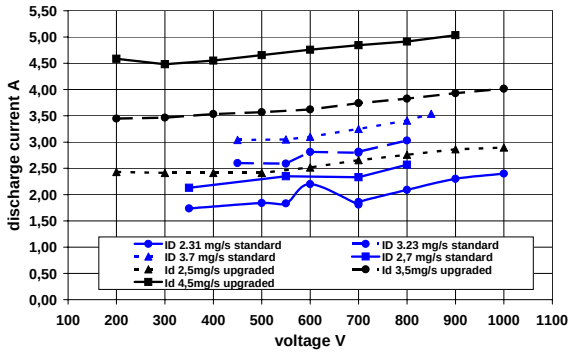

Fig. 2 Discharge current (A) as function of applied voltage (V)

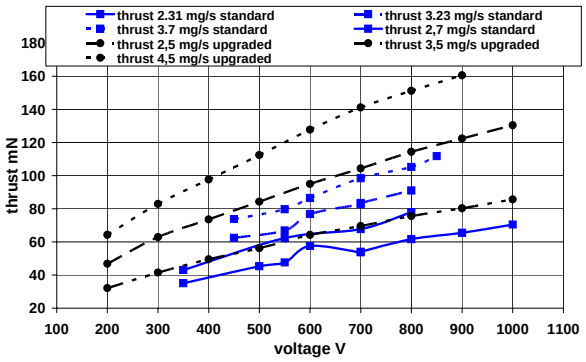

Fig. 3 Thrust (mN) as function of applied voltage (V)

2) Specific Impulse and Efficiency

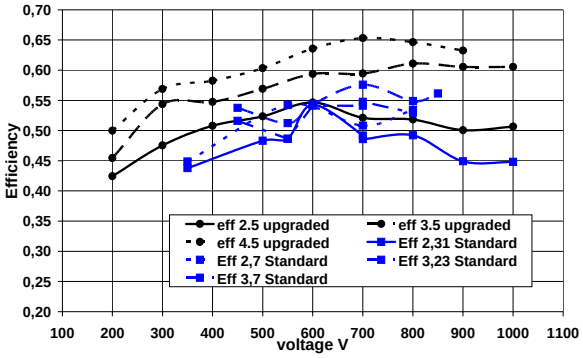

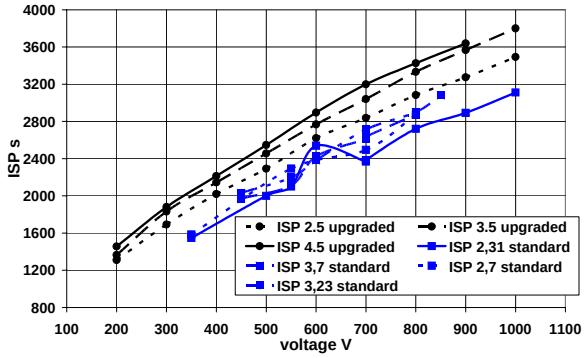

Fig. 4 Efficiency as function of applied voltage (V)
Fig. 5 Specific impulse (s) as function of applied voltage (V)

B) Direct comparison

Looking at the performances of the standard PPS thruster, an increase of the discharge current of the standard version is observed for applied voltages higher than ~600 V, as shown on **Fig. 2**. Around 600V a local enhancement of recorded values for both current and thrust coincides with the occurrence of strong oscillations of the thruster current, therefore the measurements can be less reliable. The efficiency decreases after 600 V for two mass flow rates (2.31 and 2.7), indicating a possible increase of the electronic component of the discharge current (see **Fig. 4**).
Looking at data related to the upgraded PPS version, the discharge current increases also smoothly with an increase of the discharge voltage in spite of the improved magnetic design allowing a better control of the discharge current in the whole range of operation. This discharge current is always higher than for the standard PPS-1350 at the same mass-flow rate. The efficiency and specific impulse of this upgraded version are clearly improved, especially for higher anode mass flow rate. But, as shown on **Fig. 6**, these two thrusters have similar characteristics when ISP data are referred to discharge power level. These features are discussed below.
Higher discharge current can result from two contributions: a higher electron current entering the channel or a higher contribution of multiple charge ions leaving the thruster. It can be noted that, at high voltage (>600V), the efficiency decreases more significantly at low mass flow rates. At high mass flow rate (>3mg/s), the efficiency decreases slightly for the standard version, while it seems to reach an upper limit (or to decrease less) for the upgraded version. If we suppose a high mass flow utilization efficiency, then the reduction of efficiency can come from a higher electronic contribution to the thruster current, which does not participate to the thrust but participate to the power, and/or from an increase of the doubly charged ions current. Both phenomena can vary with operation parameters: the electronic component of current can explain the increase of discharge current at low mass flow rate but at higher mass flow rate (>3mg/s) the increase of discharge current may come from two processes: electronic current and (or) the doubly charged ions current.
A rough estimation of trends in ionization efficiency will be given, for both thrusters, by the ratio between the thruster current I_d and the "anodic flow equivalent current I_m" as defined below.

$$\frac{I_d}{I_m} = \frac{I_d . M_{Xe}}{e \aleph_a \dot{m}_a}$$

This ratio, given on **Fig. 7**, shows clearly that the upgraded version has a current significantly higher than the standard one (ratio1.4 and 1.1). This ratio increases with the anode mass flow rate, for both thrusters, in agreement with an increase of the plasma density in the channel and of the ionisation probability.

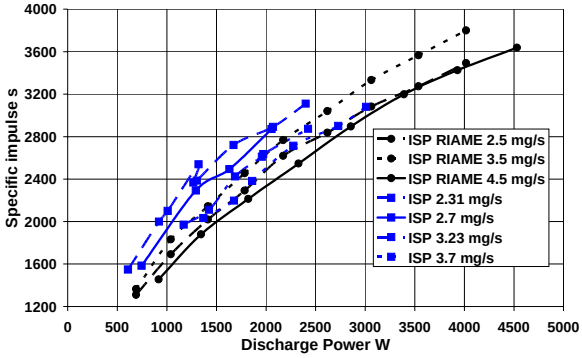

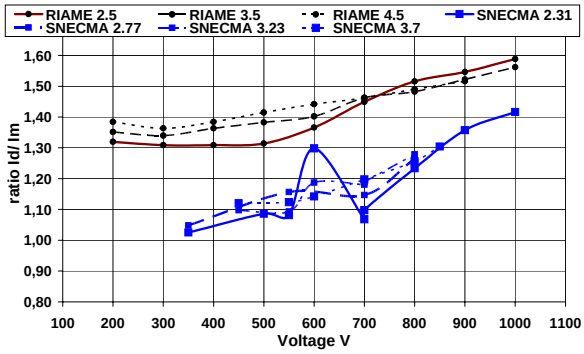

Fig. 6 Specific impulse (s) as function of discharge power (W)
Fig. 7 Discharge current over anode equivalent current as function of discharge voltage (V)

As shown above, the upgraded version of PPS-1350 presents a better Isp as function of the applied voltage than the standard version, but its specific impulse for the same discharge power is only slightly different.
We can use these results for an estimation of the energy of ions in the plume. If we assume that all ions are single charge ones, $Isp = \dfrac{T}{\dot{m}_a g}$ can be expresses as $Isp = \dfrac{\dot{m}_i^+ \left\langle v_i^+ \right\rangle}{\dot{m}_a g}$. To calculate the averaged axial ions velocity $\left\langle v_i^+ \right\rangle$ we have to take into account the spread due to the plume divergence.

We can estimate this effect by an approximation about the plume shape. If we assume an azimuthal symmetry of the plume and an absolute value of ion flux velocity varying with off-axis angle θ as $v_i^+ = v_{i0}^+ \cos(\theta)$ with v_{i0}^+ is the ion flux velocity on the axis (see Ref. 3), then the averaged axial ion flux velocity is:

$$\left\langle v_i^+ \right\rangle = v_{i0}^+ \frac{\int_0^{\frac{\pi}{2}} \Phi_i^+(\theta)\cos^2(\theta)\sin(\theta)d\theta}{\int_0^{\frac{\pi}{2}} \Phi_i^+(\theta)\sin(\theta)d\theta} = c_\theta \times v_{i0}^+ .$$

Previous studies, achieved on the RIAME thruster SPT-140ML, lead to values of c_θ close to 0.9 (see Ref. 3).
The mean kinetic energy of the ions ejected axially is

$$E_{i0} = \left\langle v_i^2(\theta = 0) \right\rangle = v_{i0}^2 + \sigma_v^2 .$$

The averaged axial ion energy has a reasonable upper limit $E_{i0} < qU_d$. Neglecting, at first approximation, the contribution of the ion velocity distribution term σ_v^2, the energy E_{i0} can be related to the Isp of the thruster (expression given above)

$$E_{i0} \geq v_{i0}^2 = \left(\frac{\left\langle v_i^+ \right\rangle}{c_\theta} \right)^2 = \left(\frac{Isp \cdot g \cdot \dfrac{\dot{m}_a}{\dot{m}_i^+}}{c_\theta} \right)^2 = E_{i\min} .$$

Therefore, for the ionization level $\dfrac{\dot{m}_i^+}{m_a}$, the following relation can be derived:

$$\left(\frac{\dot{m}_i^+}{m_a} \right)^2 \geq \left(\frac{Isp \cdot g}{c_\theta} \right)^2 \times \frac{1}{E_{i0}} \geq \left(\frac{Isp \cdot g}{c_\theta} \right)^2 \times \frac{1}{qU_d} .$$

This ionization limit is given in the Table below for the two versions of the PPS-1350, as well as corresponding E_{i0} values.. These results suggest a significant improvement of ionization and acceleration for the upgraded version.

	Mass flow, mg/s	Id, A	Ud, V	Pd, W	Isp s	E_{i0} eV	Ei/Ud	$1>\frac{\dot{m}_i}{\dot{m}_a}>$	Id/Im
Standard	2,31	2,09	800	1672	2720	604	***0,76***	***0,87***	1,14
upgraded	2,50	2,66	700	1858	2837	657	***0,94***	***0,97***	1,45

Table 1 Estimation of the ionization level between the both PPS versions

For the upgraded version the obtained ionization level and effective acceleration E_i/U_d are too high, as proved by the results obtained at higher mass-flow rate and given below.

	Mass flow, mg/s	Id, A	Ud, V	Pd, W	Isp s	E_{i0} eV	Ei/Ud	$1>\frac{\dot{m}_i^+}{\dot{m}_a}>$	Id/Im
Upgraded	3,5	3,74	700	2619	3040	754	***1,08***	***1,04 !!***	1,46

Table 2 Estimation of the ionization level at higher mass flow for the upgraded version

This analysis shows that, under the assumption of only single charge ions, ionization efficiency higher than 1 is obtained, while the ratio I_d/I_m remains constant. It means that the presence of doubly charged ions is clearly required to remove such inconsistency.

III. Model of discharge current components

A) Estimation with the performances: discharge current and thrust

A simplified model is used to estimate and predict the behaviour of the different components of discharge current (single and double charge ions, electronic current) at the exit plane of the discharge channel.

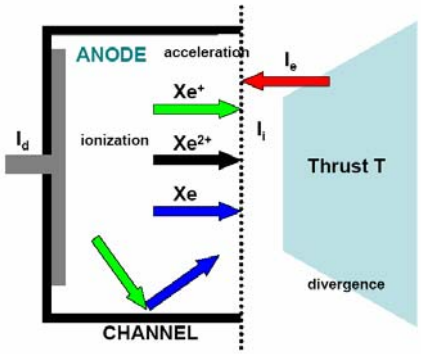

Fig. 8 Schema of the performances model

The assumptions and parameters of the model are defined below.

- We suppose the creation of single and double charge ions in the same area therefore they observe the same fall of potential: $\sqrt{2}.v_i^+ = v_i^{2+}$
- The parameter γ is an ionization efficiency coefficient: $\left(\dot{m}_i^+ + \dot{m}_i^{2+}\right) = \gamma.\dot{m}_a$
- The parameter δ ($\delta = \frac{1}{c_\theta}$) is a divergence coefficient allowing to express the thrust as : $\delta.T = \dot{m}_i^+.v_i^+ + \dot{m}_i^{2+}.v_i^{2+}$
- The discharge current is given by : $I_d = I_i + I_e = \frac{e\aleph_A}{M_{Xe}}\left(\dot{m}_i^+ + 2\dot{m}_i^{2+}\right) + I_e$

- We suppose that the ions are accelerated by an effective potential drop $U_d - \Delta U$ with ΔU of the order of 30 Volts, leading to the relation $\delta.T = \left(\dot{m}_i^+ + \sqrt{2}.\dot{m}_i^{2+}\right)\sqrt{\frac{2e}{M}(U_d - \Delta U)} = \left(\dot{m}_i^+ + \sqrt{2}.\dot{m}_i^{2+}\right)v_i^+$

Obviously, parameters γ, δ and ΔU should vary as function as the applied discharge, but here we assume that the ionization efficiency increases linearly with the voltage, ΔU is constant and δ should be better for the upgraded version because of the reduction of ions losses onto the walls and the focus of the ions beam by the improved magnetic field topology (1.11 standard and 1.05 upgraded).
Limits of the values allowed for the free parameters are defined by the requirement to derive from the model non-negative values for the various contributions of thruster current.

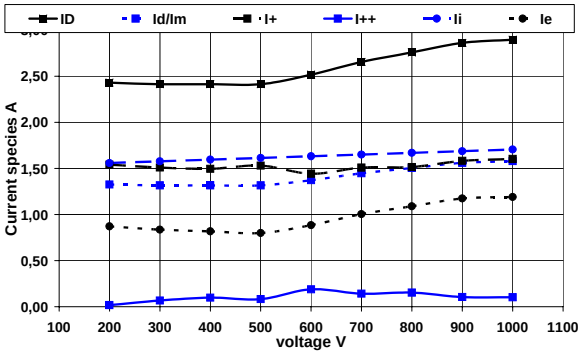

Fig. 9 Ions species 2.5 mg/s Upgraded version

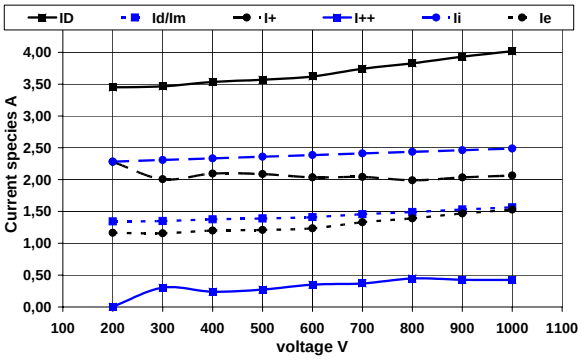

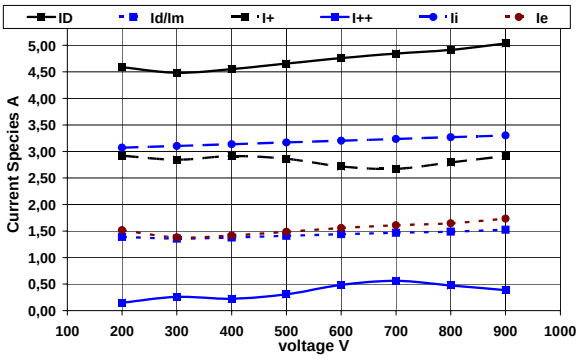

Fig. 10 Ions species 3.5 mg/s upgraded version
Fig. 11 Ions species 4.5 mg/s upgraded version

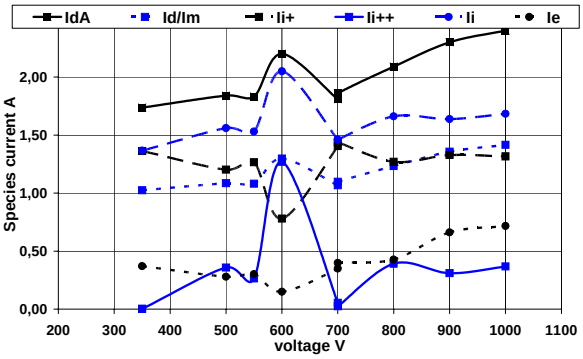

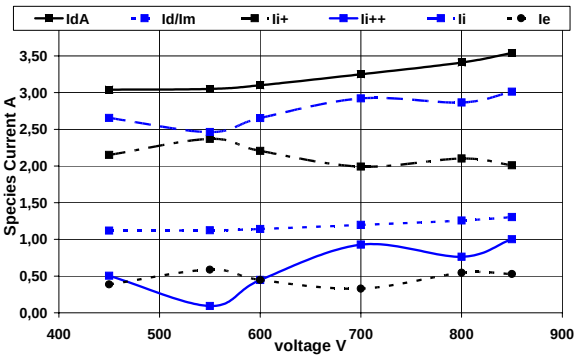

Fig. 12 Ions species 3.7 mg/s Standard version
Fig. 13 Ions species 2.31 mg/s Standard version

The model best fit with experimental data defines the single and doubly charged ions contributions which are in good agreement with the measured performances. This best agreement is obtained with an efficiency γ of ionization and a divergence δ respectively adjusted to higher and lower values for the upgraded version in comparison with best fit values for the standard version. This result point emphasizes a different behaviour of the two thrusters in term of ionization and focusing of the ion trajectories.
The increase of current in upgraded version is mainly explained by an increase of the electronic current component, especially at the lowest mass flow rate (**Fig. 9**). At higher mass flow rates 3.5 and especially at 4.5mg/s (**Fig. 10 and Fig. 10**), we note an increase of I^{2+} contribution.
The same remark can be applied for the standard version. At the lowest mass flow (**Fig. 13**), if we exclude the point at 600V, the electronic current has a strong increase which can explain the strong increase of discharge current especially at high voltage (beyond 600V). At higher mass flow, the standard version shows a better control on the discharge current increase. The both components seem to participate together at this current increase.
The standard version presents a percentage of double charged ions flow over the global ion flow null at low voltage (350V) and this percentage reaches the value of 12.3% at 1000V for the mass flow rate of 2.5mg/s. At 3.7mg/s (**Fig. 12**) this percentage starts at 10.5% for 450V and ends at 20% for 850V. The upgraded version presents a low percentage of doubled charge ions at low mass flow rate 1-6% but this contribution appears higher at higher mass flow rate (up to 17% for 3.5 mg/s , 1000V).
The above results appear consistent with the general trend of a better operation of Hall thrusters when the mass flow rate increases. They suggest a significant increase of double charge ions for higher mass flow rate and higher voltage but this result is more qualitative than quantitative, and it is not obvious to define this contribution with accuracy.

B) Comparison with measured data of ionic current by RPA

The ion flow of the PPS 1350 MLM, obtained as explained before at RIAME, is presented below.

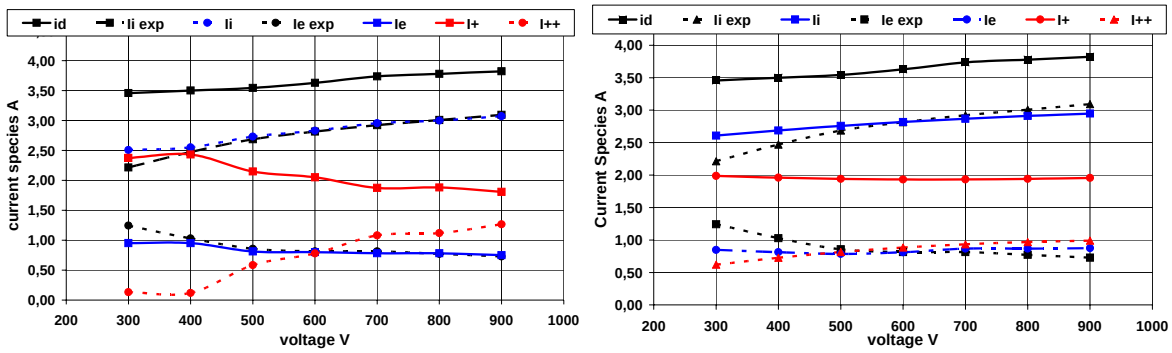

Fig. 14 Experimental measurement of I_i at 3.5mg/s (strong agreement on ionic current)
Fig. 15 Experimental measurement of I_i at 3.5mg/s (correction due to RPA measurement)

The graph (**Fig. 14**) is the results of previous model if we try to fit the measured ionic current. We observed that the part of doubly charged ions increases strongly from 2.7 to 25.9% of I_i. But it is worth to recall some drawbacks in the RPA measurements of the ion flow density. As low energy ions (< 50 eV) are not measured, we can underestimate Ii at low thruster voltage. Inversely, at high voltage (>600V), the current due to secondary emission of the RPA collector, not cancelled ion our measurements, can lead to an overestimated value for I_i. It means that, as shown on **Fig. 15**, the contribution of doubly charged ions could not present a strong increase but a smoother one, from 13% at 300V to 20% at 900V.
Even if qualitative indications are of interest, more direct insights are clearly required for a quantitative characterization of the various contributions to the current and to the plume of thrusters.

IV. Physical data for PPS-1350-MLM

A) Local parameters data

The local plasma parameters were measured under several operation modes and integral parameters were determined during the same experiments with floating probes. Results are given (**Table 3**)

$\dot{m}_a$ mg/s	Ud V	Id A	T mN	P W	Isp	Eff	Im1	Im2	Um1	Um2	Im3
3,5	300	3,46	62	1038	1807	0,529	0,96	0,73	3,64	5,572	-2,5
3,5	500	3,57	85,1	1784	2480	0,58	1,12	0,7	4,31	5,358	-2,5
2,51	707	2,68	71	1895	2890	0,531	1,04	0,98	4,32	7,624	-2,5
3,5	710	3,74	104,5	2654	3045	0,588	1,07	1,07	4,52	8,112	-2,5

Table 3 Thruster integral parameters for the chosen operation modes

The most reliable data, on probe floating potential, show that the main potential drop is realized near the accelerating channel exit (Fig 16), as in other modern SPT models. One can note also that the relative potential distribution depends on discharge voltage as well as on the magnetic field topology. The last one can be partially characterized by the ratio of the magnetization current Im1 in the internal magnetization coil and of magnetization current *Im2* in the external coils. This ratio was practically the same for operation modes with discharge voltage ~700V and larger for the 300V and even larger for 500V. Comparing these distributions, one can see that increasing the discharge voltage (under operation modes optimization) causes a shift of the accelerating layer towards the channel exit. An additional shift of potential distribution in the 500V case can be connected with significant change of the magnetic field topology, typically causing the shift of the plasma blob to the external wall in this case. One can note also that reduction of the mass flow rate under 700V discharge voltage practically does not change potential distribution under optimized operation modes.

The data on ion current distributions are represented **Fig. 17**. These distributions have well defined maxima. It is reasonable to connect these maxima with the "ionization zone" layer, more or less divided from the accelerating layers evidenced on figure 16. An increase of discharge voltage and mass flow rate lead to an increase of the ion current maxima and change of the magnetic field topology in the 500V case causes also a notable shift of the ion current density distribution.

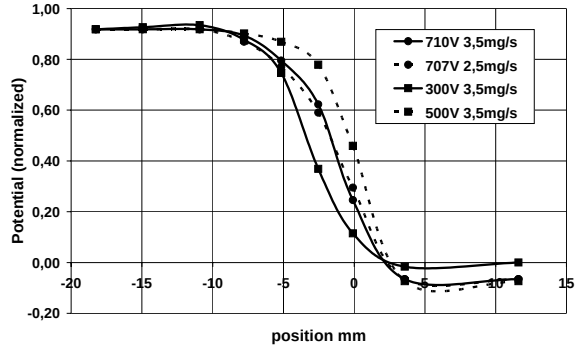

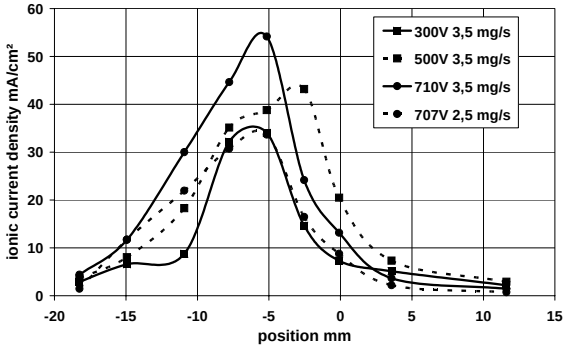

Fig. 16 Relative (divided by U_d) probe floating potential distribution along the accelerating channel
Fig. 17 Probe ion current distributions along the accelerating channel

Probe data acquired in the near anode zone (~8-20mm from the exit) are considered as reliable to derive plasma potential distribution in this near wall domain (**Fig. 18**). They show that plasma potential in the near anode zone relative to cathode potential is close to the applied voltage magnitude and is smoothly varying in the near anode zone.

In the same domain, probe data lead to electron temperature and plasma density values as shown on **Fig. 19**. A significant increase of the electron temperature is observed when the discharge voltage increases. Absolute values of the maximum values of the electron temperature are questionable: they were obtained within the accelerating layer with strong gradients of all parameters by a standard processing of "bad" probe characteristics. The most probable

option is that these maximums are overestimated at least due to relatively large probe sizes. But in the near anode zone the temperature levels seem as realistic ones and the relative significant increase of the electron temperature is well correlated with the density increase in the near anode zone. These data on electron temperature ~(6-8)eV are in agreement with critical ones required to achieve an efficient enough ionization in this zone and the observed increase of electron temperature level can explain also the increasing fraction of multiply charged ions when the thruster voltage increases, as deduced from data on current and thrust in the PPS-1350 MLM.

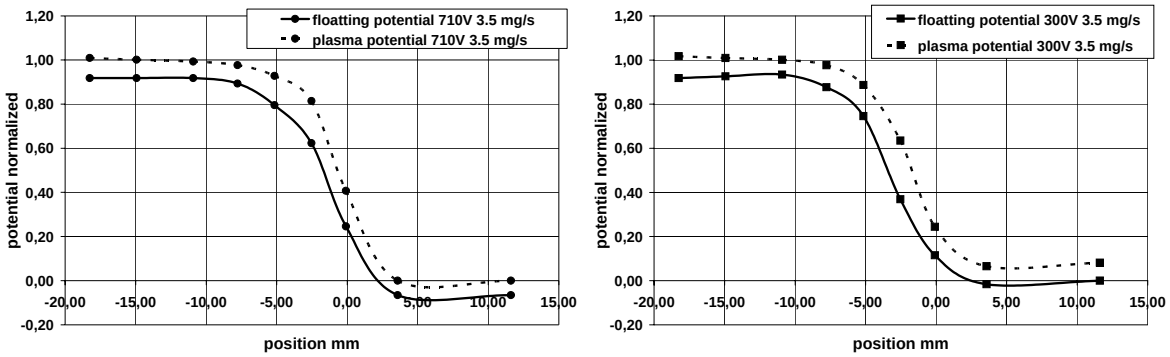

Fig. 18 (a) 700V (b) 300V Plasma potential distributions along the accelerating channel

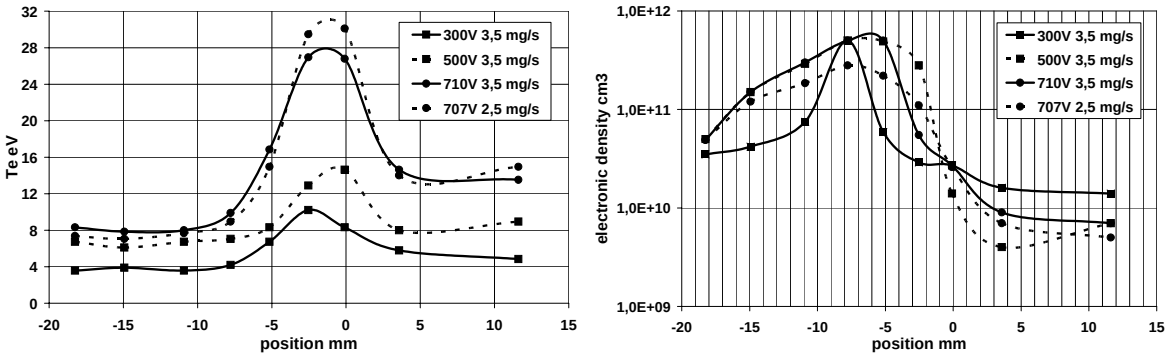

Fig. 19 (a) Electron temperature distributions & (b) plasma density along the accelerating channel

Summarizing the results of the local plasma parameter measurements general trends have been evidenced when increasing the thruster voltage:

the ionization zone increases into the both direction towards the anode and the exit of the channel, then the ionization efficiency is increased; as all ions do not see the same potential drop their energy dispersion should increase.
the electron temperature is increased and the increase of the plasma density in the near anode zone can also explain an increase of the doubly charged ions fraction in the PPS-1350 ML.

V. Simulation results

A) Model and method

The 2D hybrid code developed by L.Garrigues et al.[8-9] has been applied for simulating the thruster behavior at high voltage. This code is based on an axisymetric, two-dimensional (r, z), model of the thruster. The simulation domain includes the discharge channel and a near output area which extends on ~5 cm into the plume. The magnetic field is adjusted to experimental data. Neutrals, single and double charge ions are described by a Monte-Carlo simulation. Double charge ions are assumed to be produced both from the atom and single charge ion ground states. Electric field is calculated from the electron transport equations. The electron mobility in the channel is modeled with the use of momentum-transfer frequency induced by electron-particle collisions and wall collisions, i.e.

$$\mu_\perp = \frac{m_e}{eB^2}(\nu_{m,particles} + \nu_{walls}) = \frac{m_e}{eB^2}(\nu_{m,particles} + \alpha\nu_{ref}) = \mu_{\perp,c} + \alpha\left(\frac{m_e\nu_{ref}}{eB^2}\right)$$

where α = 0.1-2 is a constant fitting parameter, $\nu_{ref} = 10^7$ s^{-1}. Outside the channel, a Bohm-like "anomalous" conductivity is considered and the electron mobility is described as:

$$\mu_\perp = \mu_{\perp,c} + \frac{K}{16B}$$

where K=0.1-2 is also a fitting parameter. The phenomenological expression describing electron energy loss is:

$$W = \alpha_\varepsilon \times 10^7\, \varepsilon \exp\left(-\frac{U}{\varepsilon}\right)$$

where α_ε=0.1-1 and U=20 eV are once again fitting parameters, and ε is the electron energy. A detailed discussion of the model can be found in Ref. 8-9.

B) Simulation results and discussion

Two operation modes were simulated: $\dot{m}_a$ = 3.5 mg/s, U_d = 500 V and $\dot{m}_a$ = 2.5 mg/s, U_d = 700 V (**Table 4**). The mass flow rate used in the simulations was increased by 5% relative to experiments (suspected deviation of the flow-meter indication).

The code was able to give both discharge current and thrust values within 5% agreement with the experimental data for the first operating point : $\dot{m}_a$ = 3.5 mg/s (3.675 mg/s in simulation), U_d = 500 V (see **Table 4**),. The simulation predicts a contribution of electron current of ~17 %, and a noticeable contribution of double charge ions : ~8 % of the total current, i.e. ~10% of the total ion current. The calculated ion current ($I^+ + I^{++}$) is close to the measured value (see **Fig. 20-24** and **Table 4**).

For the second operation mode $\dot{m}_a$ = 2.51 mg/s (2.636 mg/s in the simulation), U_d = 700 V, the code predicts discharge current, ion current and thrust lower than the measured ones. Some time-averaged distributions of local parameters in the channel, along the channel wall (R = 50 mm) and on middle radius (R = 43 mm) are presented in **Fig. 20-24.**

The code leads to calculated distribution of plasma potential near the external wall (see **Fig. 20 b**) close to the measured one. The calculated axial distribution of the electron energy $E_e = \frac{3}{2}T_e$ (see **Fig. 21b**) is qualitatively similar to the experimental distribution, in particular for the location of the maximum value in the channel. But a significant discrepancy seems to be evident for the absolute values: the maximum measured electron temperature value is $\frac{3}{2}T_e$ = 45 eV, whereas the maximum calculated value is 75 eV. In fact the near wall probes give mainly an information on the electron energy distribution along one direction (the local magnetic field line) while the code gives the total electron energy and the difference of data is more likely within the uncertainties of electron energy determinations.

The single charge (Xe^+) ion density is, by one or two order of magnitude, much higher than the double charged one (see **Fig. 20-24**). Therefore, the Xe^+ density is well representative of the plasma density in the channel. The simulation predicts a high density in the near-anode region z ≈ 5 mm, whereas the measured maximum value is located at z ≈ 12 mm, i.e. closer to the channel exit. Such a high gap between the region of Xe^+ maximum density and the region of high electron energy can explain an underestimation of the double charged ion fraction in the simulation. In turn, a lower Xe^{++} fraction could also explain the lower thrust and lower ion current predicted by code.

The most general trend confirmed by both simulation and experiments is the increase of electron energy when the discharge voltage increases (see **Fig. 21**). Inversely the conclusion of an increasing contribution of double charge ions, derived from experimental data, is not evidenced by the simulation. It is clear, again, that further investigations, both experimental and numerical, remain necessary to clarify this point in a quantitative way.

Table 4 PPS®1350Upgraded performance for different combinations of electron transport parameters

Electron transport coefficients			Thruster macroscopic characteristics						
k_b	k_α	k_ε	$\dot{m}_a$, mg/s	I_d, A	I^+, A	I^{++}, A	Ie, A	F, mN	E_{emax}, eV
U_d = 500 V									
Experiment			3.5	3.55	2.7			83.5	22
0.2	1	0.7	3.675 (+5%)	3.43	2.58	0.28	0.57	84.5	50
U_d = 700 V									
Experiment			2.51	2.68	2.2			71.0	45
0.2	1	0.7	2.636 (+5%)	2.26	1.8	0.2	0.26	67.6	75

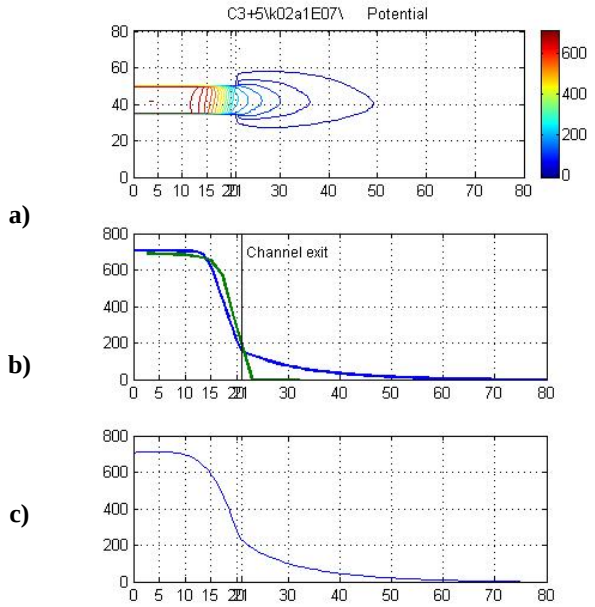

Fig. 20 Potential, V, a) in the channel and outside; b) on the external wall; c) on R=43 mm.

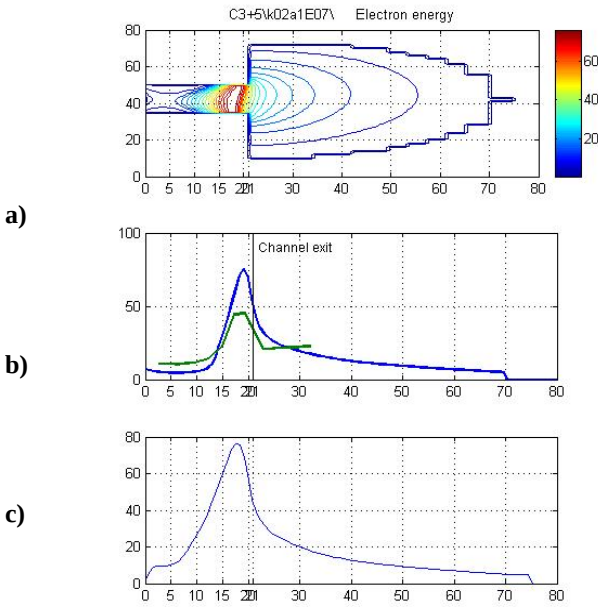

Fig. 21 Electron energy, eV, a) in the channel and outside; b) on the external wall; c) on R=43 mm.

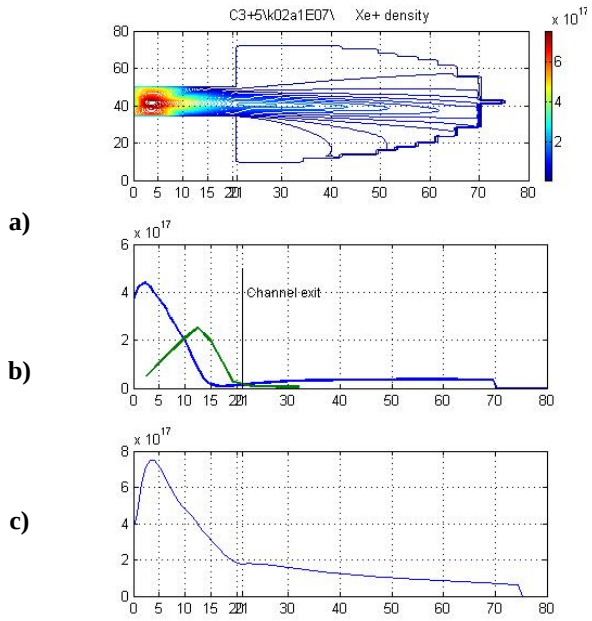

Fig. 22 Xe^{+} density, m^{-3}, a) in the channel and outside; b) on the external wall; c) on R=43 mm

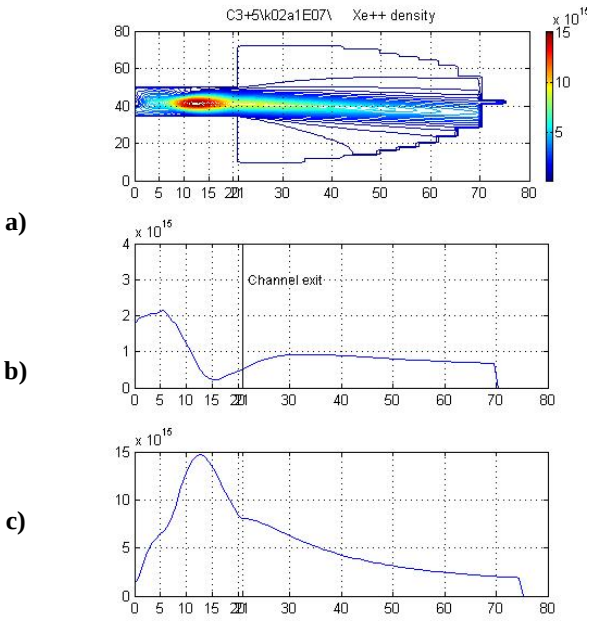

Fig. 23 Xe^{++} density, m^{-3}, a) in the channel and outside; b) on the external wall; c) on R=43 mm;

Conclusion

A standard and an upgraded version of the thruster PPS-1350 have been characterized in a voltage range extended till 1000 Volts. The measured performances are better in term of thrust for the upgraded version, characterized by an improved magnetization intensity and morphology. But efficiency and specific impulse (~2900s for 3kW) are almost the same especially if we study performances as function of the discharge power for the operation modes of constant discharge power.

A specific impulse of 3000s can be reached with a PPS-1350 but the lifetime at this operating point of 700V seems to be difficult because of the lowering of efficiency and the erosion of ceramic walls.

An higher discharge current is observed in the upgraded PPS-1350 MLM thruster, reasonably related to the contribution of double charge ions and a better ionization. Nevertheless, especially at the lower mass flow rate, the possible impact of an increase of the electronic current component of discharge current can not be neglected.

The measurement of the total ionic current in the plume is always difficult at high angles. Moreover as we saw it is not obvious to determine the part of double and single charge ions only from the performances data. So we need additional inputs (mass spectrometry or time of flight techniques) to confirm the ratio of their contribution and, perhaps, add some insights on their creation zone. This last information is related to the processes of creation and to the divergence of the Xe^{2+} ion beam in the plume.

Some results of simulation, obtained with the 2D hybrid code of CPAT, show some discrepancies with experimental data, obtained at high discharge voltage, such as ions density and electron energy. Nevertheless, the code confirms the trend, at high thruster voltage, of increasing electron energy and an expanding ionisation area. But the experiment suggests a broadening in both directions (towards anode and channel exit) while the code suggests an extension towards channel exit.

To summarize, this exploration of performances of both PPS-1350 versions, till discharge voltages as high as 1000 volts, suggests that this operation of ISP Hall thrusters represents a realistic goal. Nevertheless further investigations remains required, both in term of physics and design, for an optimisation of high specific impulse, high efficiency and long life time structures.

Acknowledgements

Thanks for their financial support to the CNES, SNECMA, and the INTAS program. A special thank for all Russian and Ukrainian teams involving in the INTAS program.

References

[1]V. Kim, G. Popov, B. Arkhipov *et al*, in *Proceedings of the 27th International Electric Propulsion Conference, Pasadena, USA, 2001* (Electric Rocket Propulsion Society, Worthington, OH, 2001), IEPC-01-05.
[2]G.D. Racca, in *Proceedings of the 4th International Spacecraft Propulsion Conference*, Sardinia, Italy, 2004 (ESA Publications Division, 2004).
[3]A. Lazurenko, V. Vial A. Bouchoule, A.Skrylnikov, V. Kozlov, V. Kim ***Dual mode operation of stationary plasma thrusters,*** AIAA J. Propulsion Power (accepted)
[4]Richard Hofer, ***Development and characterization of high efficiency, high specific impulse xenon Hall thruster***, PhD dissertation, University of Michigan 2004
[5]R. Hofer, A. D. Gallimore, ***Efficiency analysis of a high specific impulse hall thruster***, AIAA-2004-3602
[6]Manzella, D.H., Jacobson, D.T., Jankovsky, R.S., "**High Voltage SPT Performance**", *37th Joint Propulsion Conference and Exhibit*, paper AIAA-2001-3774, USA, 2001
[7]Pote, B. and Tedrake, R., "**Performance of a high Specific Impulse Hall Thruster**", *27th International Electric Propulsion Conference*, paper IEPC-01-35, USA, 2001
[8]Hagelaar, Bareilles, Guarrigues and Boeuf, ***Two dimensional model of a stationary plasma thruster,*** J. Appl. Phys. 91, 5592 (2002)
[9]Hagelaar, Bareilles, Guarrigues and Boeuf ***Role of anomalous electron transport in a stationary plasma thruster simulation,*** , J. Appl. Phys. 93, 67 (2003)
[10]M.Prioul, F.Marchandise, P.Dumazert et al "**PPS®-1350 qualification status and performances**", 4th International Spacecraft Propulsion Conference, Sardinia, Italy, 2004
[11]V. Vial, A. Lazurenko, A. Bouchoule, M. Prioul, L. Garrigues, J.–P. Bœuf, **PPS®1350-G in an extended operation domain : comparison between experimental and simulation results**, 50th Joint Propulsion Conference and Exhibit, AIAA-2004, July 11-14 Ft. Lauderdale, FL, USA, 2004
[12]A. Bouchoule, A. Cadiou, A. Heron, M. Dudeck, and M. Lyszyk, "**An overview of the French research program on Plasma Thrusters for Space Applications**", Contrib. Plasma Phys. **41** (6), 573 (2001)